Reviewed research article

Dense seismic network provides new insight into the 2007 Upptyppingar dyke intrusion

Hilary R. Martens[1], Robert S. White[1], Janet Key[1], Julian Drew[1], Heidi Soosalu[1,2] and Steinunn S. Jakobsdóttir[3]

[1]*Bullard Laboratories, University of Cambridge, Madingley Road, Cambridge CB3 0EZ, UK*

[2]*Geological Survey of Estonia, Kadaka tee 82, Tallinn 12618, Estonia*

[3]*Icelandic Meteorological Office, Bústaðavegur 9, 150 Reykjavík, Iceland*

hilarymartens@gmail.com, rsw1@esc.cam.ac.uk, ajk65@cam.ac.uk, drew2@slb.com, heidi@hi.is, ssj@vedur.is

Abstract — *Factors such as network geometry, network size and phase-picking accuracy have significant effects on the precision of seismic hypocentre locations. In turn, the precision of the hypocentral locations dictates the degree to which morphological details within seismic swarms may be resolved. The Icelandic national seismic network (SIL) is designed to monitor seismic activity across large expanses of Iceland in real-time using automated earthquake detection and location software. Here we examine the performance of the SIL network relative to a much denser, local network of seismometers deployed around the Askja volcano in the Northern Volcanic Zone. A subset of earthquakes from the 2007–2008 dyke intrusion beneath Mt. Upptyppingar is used to compare single- and multi-event hypocentral locations. Specifically, we highlight 288, high signal-to-noise ratio events that occurred during an intensive sequence of earthquakes from 6–24 July 2007, when the temporary Askja network was active. A careful refinement of phase onsets recorded by our well-configured, dense network of receivers reveals hypocentres clustered tightly on a planar structure, interpreted as a dyke dipping at 49°. The root-mean-square (RMS) misfit to the plane (114 m) is only slightly greater than the uncertainties in relative locations of the earthquakes themselves, and constitutes a three-fold reduction in RMS misfit over SIL relative locations. The improved precision, facilitated predominantly by a more favourable network size and configuration, permits a more detailed analysis of the intrusion.*

INTRODUCTION

Between February 2007 and April 2008, intensive episodes of micro-seismic (local magnitude (M_l) < 2.2) activity were recorded near Mt. Upptyppingar in the northwestern part of the Kverkfjöll volcanic system in Iceland's Northern Volcanic Zone. A map of the study area is shown in Figure 1. The seismicity occurred primarily in swarms of tens to hundreds of earthquakes clustered tightly in space (within tens to hundreds of metres) and time (within minutes to hours), and delineates a southward dipping planar structure as shown in Figure 2. The spatial coherency of the hypocentres, supplemented by surface deformation recorded by continuous GPS, led Jakobsdóttir *et al.* (2008) to propose that the seismicity was caused by melt intrusion in a dyke.

The Upptyppingar swarms locate at depths of 13–19 km below sea level, which is well beneath the local brittle-ductile boundary at 6–7 km depth (Soosalu *et al.*, 2010) and above the estimated Moho depth at 25–30 km (Darbyshire *et al.*, 2000). Despite their origin in ductile crust, however, the earthquakes exhibit frequency content similar to tectonic earthquakes at shallower levels. Brittle failure in ductile crust re-

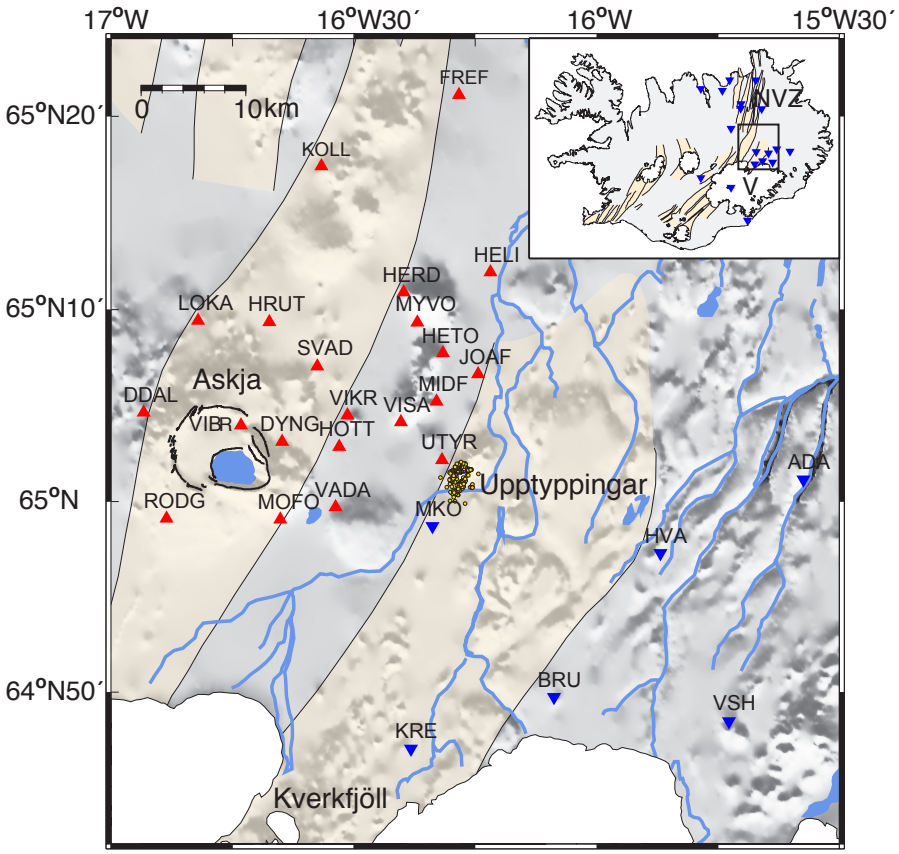

Figure 1. Map showing the network of 21 Cambridge University instruments (upright red triangles) plus six SIL stations (inverted blue triangles) that comprise the Askja Seismic Network (ASN). Inset shows the maximum number of SIL network instruments used by IMO to locate hypocentres during July 2007. The Cambridge University station DYNG has been connected to the SIL network as station ASK. The white areas in the south of the main map are part of the Vatnajökull ice cap (labelled 'V' in the inset). The Northern Volcanic Zone (labelled 'NVZ' in the inset) extends from the Vatnajökull ice cap north to the coast in a series of volcanic fissure swarms, indicated by the beige shading. Epicentres for the 6–24 July 2007 Upptyppingar events are shown as yellow dots. – *Kortið sýnir 21 jarðskjálftamælistöð í neti Cambridge háskóla (rauðir þríhyrningar) og 6 SIL-stöðvar (bláir þríhyrningar). Saman kallast netin "Askja Seismic Network" (ASN). Á innfelldu myndinni sjást allar stöðvarnar, sem notaðar voru í SIL-kerfinu til að staðsetja skjálftana í júlí 2007. Cambridge stöðin DYNG var seinna tengd SIL-kerfinu undir nafninu ASK. Nyrðra gosbeltið (NVZ á innfelldu myndinni) er í ljósbrúnum lit, Vatnajökull (V) hvítum. Upptök skjálftanna 6.–24. júlí eru sýnd með gulum doppum.*

quires high strain rates (Rubin and Gillard, 1998) that Jakobsdóttir *et al.* (2008) suggest are generated by the melt intrusion. This supposition is corroborated by measurements of surface deformation that are consistent with the inflation of a dipping dyke at mid-depth in the crust (Hooper *et al.*, 2009).

The seismic locations reported by Jakobsdóttir *et al.* (2008) are derived from data acquired by the SIL (originally an acronym for South Iceland Lowland) system. SIL has served as Iceland's national seismic network since 1991 and is designed to acquire high-quality data for earthquake prediction research and to

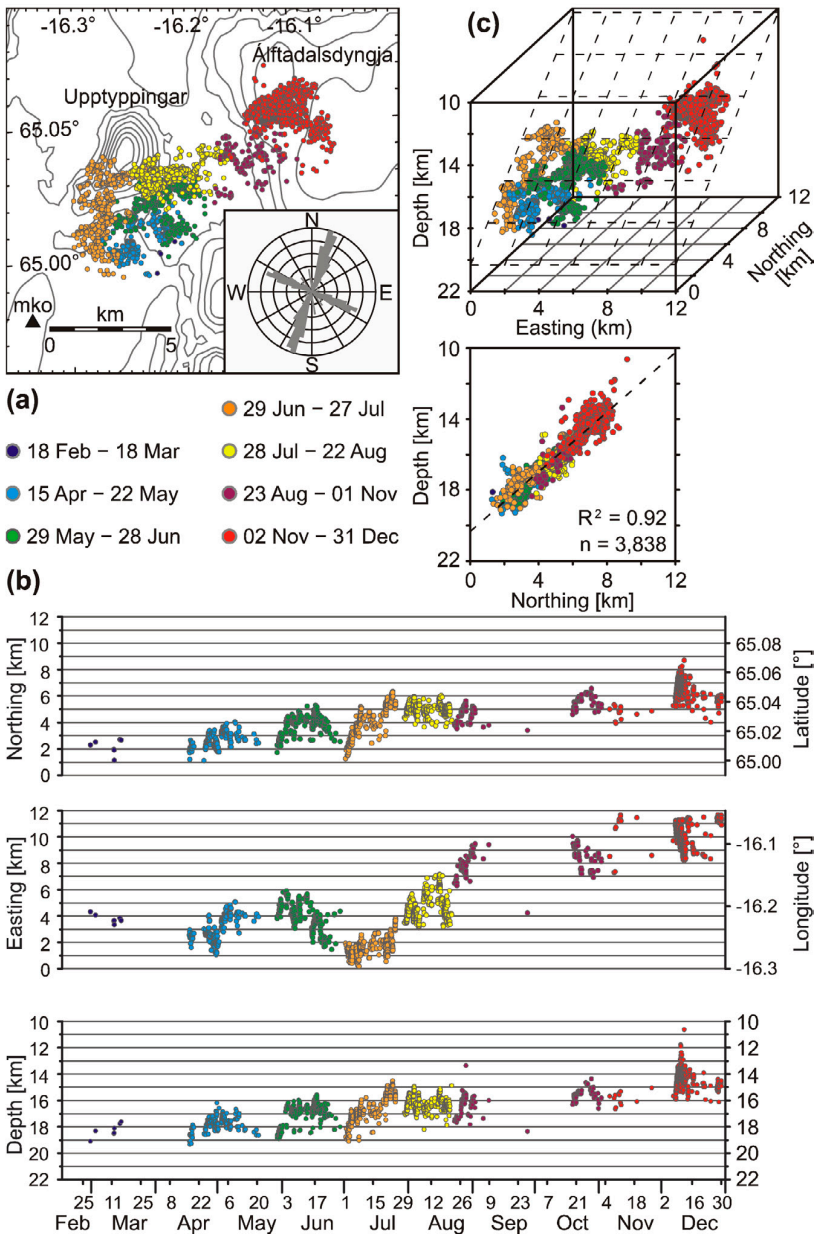

Figure 2. Distribution of Upptyppingar seismicity that occurred between 18 February and 31 December 2007 in (a) map view, (b) easting, northing, and depth, and (c) 3D, with the best-fit plane displayed from two vantage points. Figure from Jakobsdóttir *et al.* (2008). – *Dreifing jarðskjálfta í Upptyppingahrinunni frá 18. febrúar til 31. desember 2007 (a) á korti (b) breidd, lengd og dýpi, sem fall af tíma (c) í þrívídd séð frá tveimur mismunandi hornum. Á mynd (b) og (c) er hnitakerfið miðað við flötinn, sem fellur best að skjálftavirkninni. Myndin er úr grein Steinunnar S. Jakobsdóttur og fleiri (2008).*

monitor regional seismicity by computing locations, magnitudes, and focal mechanisms of seismic events automatically and in near real-time (Böðvarsson *et al.*, 1996, 1999; Stefánsson *et al.*, 1993). By the end of 2007, the network comprised 51, three-component seismometers deployed across the whole of Iceland (Jakobsdóttir, 2008). All SIL seismic data is recorded at 100 samples per second.

The SIL network is operated and maintained by the Icelandic Meteorological Office (IMO). Seismic hypocentres computed by the SIL-system's automated detection and location software are published on the IMO website, typically within minutes of an event. All locations are then manually assessed and revised as necessary (e.g., for poor time picks and false events). Phase arrival selections are refined interactively and locations are subsequently recomputed prior to publication on the 'weekly overview' section of the IMO website (hraun.vedur.is/ja/viku).

The SIL system also has the capability to derive relative locations using a double-difference method (Slunga *et al.*, 1995). The double-difference algorithm minimises travel time residuals between neighbouring events recorded at the same station; hence, it alleviates the need for station corrections for near-surface variations or deviations from the assumed one-dimensional velocity model away from the hypocentral region, with the potential for some loss in absolute location accuracy.

References to SIL in this manuscript imply the processing of SIL data using IMO techniques, unless explicitly stated otherwise.

In summer 2007, Cambridge University deployed an independent, dense network of seismometers in the vicinity of Mt. Upptyppingar to monitor lower crustal seismicity around Askja volcano (Soosalu *et al.*, 2010). The temporary network was active between 6 July and 22 August 2007 and consisted of 21, three-component Güralp 6TD broadband seismometers (Figure 1). For the analysis detailed in this manuscript, we have also included data from six nearby SIL stations (MKO, HVA, BRU, KRE, ADA, and VSH). Deployed in 2004 to monitor the formation of the nearby Hálslón water reservoir, the six SIL stations provide additional coverage east of Mt. Upptyppingar. This collective network of 21 Cambridge University instruments plus six SIL stations will henceforth be referred to as the ASN, for Askja Seismic Network (Figure 1). All instruments in the ASN record at 100 samples per second.

The Upptyppingar swarms represent the most intensive and persistent seismic activity ever recorded in Iceland's lower crust. The unique spatial morphology and temporal progression of the seismicity have the potential to shed light on crustal formation and the dynamics of dyke propagation in ductile crust. Here we examine a subset of events from the Upptyppingar dyke intrusion using data acquired by the ASN and compare our location results to those obtained using SIL data alone. We conclude with discussions on SIL system performance, the value of dense, local networks, and a geophysical interpretation of the Upptyppingar swarms.

SEISMIC OBSERVATIONS OF ACTIVE DYKES

The movement of melt within the crust, delineated by the spatial and temporal progression of seismicity, is frequently observed in Iceland. Some of the clearest examples of dyke intrusion are associated with the deflation of the Krafla volcano in northern Iceland in the late 1970s. Earthquakes were observed to migrate away from the Krafla volcanic centre at rates as high as 0.5 m s^{-1}, progressing laterally along narrow vertical channels interpreted as dykes (Brandsdóttir and Einarsson, 1979; Einarsson and Brandsdóttir, 1980).

Similar events have been observed along the rift zone in Afar (Wright *et al.*, 2006) and near Mt. Kilauea volcano in Hawaii (Rubin and Gillard, 1998). All of these observations, however, involve the migration of seismicity through the brittle, near-surface crust. Seismicity suggestive of melt movement through deeper crust is less common, but has been observed on several occasions.

In addition to Mt. Upptyppingar, seismicity delineating a planar structure in ductile crust was observed beneath Lake Tahoe in the western United States in 2003–2004 (Smith *et al.*, 2004). The Tahoe swarms occurred at 29–33 km depth, well below the local

brittle-ductile boundary of 15–18 km, along a presumed dyke that dipped at 50°.

Deep seismic activity attributed to melt movement is also observed beneath active volcanic centres in Iceland, as well as elsewhere in the world such as Mt. Kilauea (Wright and Klein, 2006) and Japan (Hasegawa *et al.*, 1991), but the hypocentres typically assume conduit-like as opposed to planar distributions.

Near Mt. Upptyppingar, hundreds of lower crustal earthquakes have been observed beneath Askja volcano since the ASN began monitoring the area in 2005 (Soosalu *et al.*, 2010). The seismicity outlines three separate vertical conduit structures that extend from c. 10 km down to the crust-mantle boundary. The most recent eruption at Askja volcano occurred in 1961.

Mt. Eyjafjallajökull in southwest Iceland also exhibited deep seismicity in the mid-1990s that extended from the crust-mantle boundary through to the surface (Hjaltadóttir *et al.*, 2009). Seismic activity persisted at shallower depths with sporadic deep events for over a decade, eventually leading to an eruption in 2010 that halted European air traffic for several days (Sigmundsson *et al.*, 2010; Hjaltadóttir *et al.*, 2009; Pedersen and Sigmundsson, 2004, 2006).

GPS and InSAR modelling of surface deformation at Mt. Upptyppingar in 2007–2008 constrain the volume of injected melt to be ∼0.040–0.047 km^3, corresponding to the inflation of a ∼0.1–1 m thick, southward dipping dyke at depths of 10–18 km (Hooper *et al.*, 2009). For comparison, the inferred volume of the pre-eruptive melt intrusion beneath Eyjafjallajökull was of the same magnitude (Sigmundsson *et al.*, 2010).

Seismicity that clearly defines a planar structure, as observed beneath Mt. Upptyppingar, presents an ideal opportunity to evaluate the effects of different processing techniques, network size and geometries, and phase picking accuracy by comparing hypocentral location precision. This form of analysis has been applied successfully in previous studies that, for example, demonstrate the benefits of relative relocation techniques (Waldhauser and Ellsworth, 2000; Slunga *et al.*, 1995).

The precision of seismic hypocentre locations affects how the seismicity is interpreted. Outstanding questions in crustal formation, such as the extent of host rock deformation caused by an active dyke intrusion in visco-elastic crust, require extremely high hypocentral precision.

ASN PROCESSING TECHNIQUES

Data selection is primarily limited by the deployment dates of the ASN (i.e., 6 July–22 August 2007). Within this date range, we further restrict our study period to 6–24 July, during which the most intensive and dynamic bursts of seismic activity occurred, including several earthquakes that exceeded M_l 2.0 and seismic propagation rates that reached as high as 0.05 m s^{-1}. Moreover, signal to noise ratios were higher on average during this period than in late July and August. The study period comprises 547 events that are drawn from a SIL catalogue of over 9000 earthquakes observed beneath Mt. Upptyppingar during 2007–2008. We then manually filtered the 547 events based on signal-to-noise ratio by inspecting waveforms for clarity of phase onsets. The final dataset consists of 288 high-quality events.

Processing of seismic data from the ASN is performed in multiple steps. Firstly, events are located using the Coalescence Microseismic Mapping (CMM) software developed by Drew (2010). The SIL event catalogue is provided as input to CMM, which searches the continuously recorded data for phase onsets near each catalogue event time through a Short Term Average to Long Term Average ratio (STA/LTA) (Drew *et al.*, 2005). For a given search volume of discrete grid spacing and a specified velocity model, a look-up table is produced by forward-modelling travel times from each grid node to each receiver. The look-up table is then used to migrate seismic energy from both P-wave (vertical component) and S-wave (horizontal components) onsets at each station into the subsurface. Finally, a coalescence function is used to determine the subsurface location at which the seismic energy is focussed, yielding spatial and temporal information about the imaged seismic event. Any mis-identified onsets (e.g., from noise bursts) are smeared out over the migrated volume and thus do not contribute to the final CMM locations. Here we have used a grid spacing of 300 m; however, by virtue of

the imaging method, final hypocentral locations are not limited to individual grid points.

In an extension to CMM, we load waveforms into an interactive phase-picking tool (PPICK), initially aligned by automatically determined CMM onset times. As illustrated in Figure 3, PPICK allows the user to make fine adjustments to arrival times prior to event relocation through a combination of event gather and station gather modes. A variety of zoom functions as well as an adjustable band-pass filter improve the ease with which phase arrivals may be identified. We estimate that PPICK facilitates the selection of high-quality Upptyppingar phase onsets to one tenth of the dominant period of the arrival (i.e., to ∼0.01 s).

Manually refined picks are generally slightly earlier than the automated times produced by the CMM algorithm because CMM locates events based on energy onsets as opposed to first arrivals. Weights of integer values between 0 and 4 are manually assigned to each arrival within PPICK based on confidence in the pick. Single-event locations are then derived using HypoInverse-2000 (Klein, 2002) and subsequently relocated relative to neighbouring events using HypoDD, a double-difference algorithm (Waldhauser and Ellsworth, 2000; Waldhauser, 2001).

References to ASN in this manuscript imply the processing of ASN data using the aforementioned processing techniques.

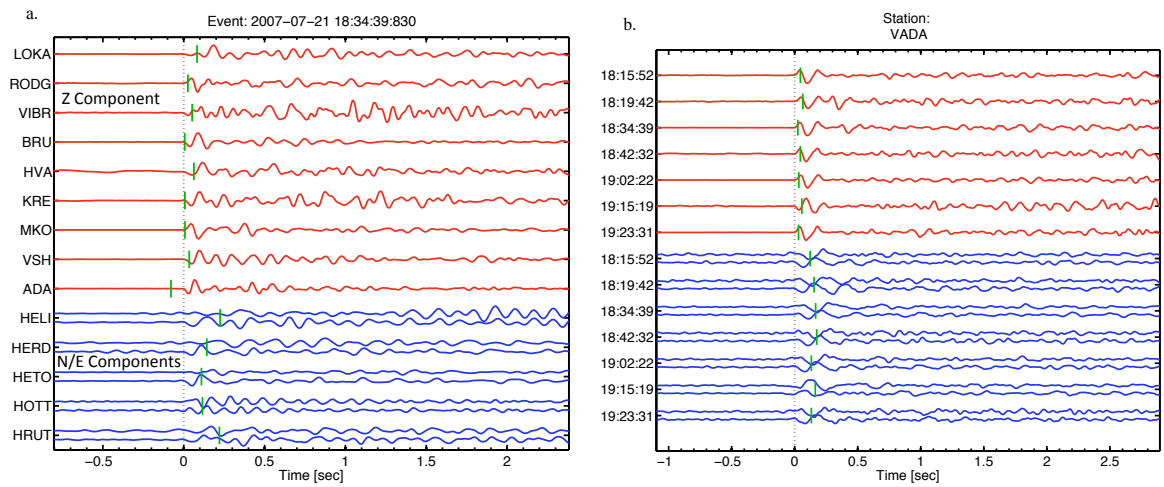

Figure 3. Panel (a) presents continuous waveform data as a PPICK event gather for an earthquake that occurred at 18:34:40 GMT on 21 July 2007 (M_l 1.8). Panel (b) depicts a PPICK station gather from VADA (for location see Figure 1) for a swarm of earthquakes that occurred between 18:15:52 GMT and 19:23:31 GMT on 21 July 2007. Red traces are Z-component and used to select P-wave arrivals. Pairs of blue traces are used to select S-wave arrivals; the upper trace is E-W component and the bottom trace is N-S component. Signals are aligned by manual time pick, band-pass filtered at 2–16 Hz, and normalised to the same peak-to-peak amplitude. The green bars indicate CMM model time picks. – *(a) Skjálftabylgjur frá mismunandi stöðvum klukkan 18:34:40 þann 21. júlí 2007 (M_l 1,8). (b) Bylgjugögn frá stöðinni VADA sem sýnir nokkra skjálfta á tímabilinu 18:15:52–19:23:31 þann 21. júlí 2007. Rauðar línur tákna Z-þáttinn, þar sem komutími P-bylgna er lesinn, en bláu pörin sýna N-S og A-V þættina, þar sem S-bylgjan er lesin. Handvirkt ákveðinn komutími bylgjunnar er settur sem núll, gögnin síuð á tíðnibilinu 2–16 Hz og stærsta útslag sett jafnt á öllum rásum. Grænu merkin sýna komutíma samkvæmt CMM staðsetningu.*

LOCATION RESULTS

To illustrate the effects of processing techniques, network geometry, network size, and phase-picking precision on hypocentral locations, we highlight five individual earthquake clusters that occurred from 20–24 July 2007 and that represent 154 of the 288 events in our study period. Courtesy of the IMO, we have access to SIL-system manually refined time picks for each event in the dataset as well as double-difference locations and uncertainty estimates. Catalogue locations produced by the SIL system's automated location software and reviewed manually are available to the public on the worldwide web and are also presented here.

All locations described in this manuscript are derived using the IMO's linear-gradient Vatnajökull velocity model. The Vatnajökull model, shown in Figure 4, is based on extrapolation from the ICEMELT refraction profile (Darbyshire *et al.*, 1998, 2000). Although most SIL on-line catalogue locations are derived using the standard SIL model (Stefánsson *et al.*, 1993; Hjaltadóttir *et al.*, 2009), locations in the Upptyppingar area default to the more locally suitable Vatnajökull model.

I. Catalogue locations

We begin with an examination of CMM output compared with on-line SIL catalogue locations. Firstly, it is important to note that SIL catalogue locations are computed with respect to the elevation of the nearest one or two seismic stations to an event. For Upptyppingar, this value is approximately 700 m; however, the offset could be substantially greater in regions with higher station elevations. Furthermore, the SIL catalogue locations are derived using data from up to 18 SIL stations. The CMM locations are derived using data from the ASN (i.e., 21 Cambridge University instruments plus six nearby SIL stations).

In Figure 5, we display the positions of SIL catalogue locations relative to the output of CMM as directly reported by each method. A systematic offset in depth is apparent; however, since CMM locations are reported as depth below sea level and SIL catalogue locations are reported as depth beneath the average elevation of the nearest receivers, the SIL locations appear 700 m deeper relative to the CMM locations than they ought to. A correction of 700 m, however, does not account for the entire offset in depth (Table 1, first column). We also note that the CMM locations, which are derived from ASN data, are noticeably tighter than the SIL catalogue locations, particularly in northing and depth.

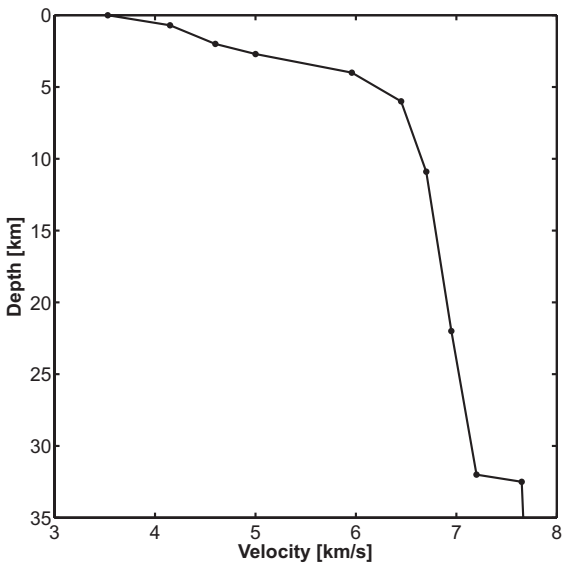

Figure 4. One-dimensional P-wave velocity model used to locate hypocentres. The linear-gradient, 'Vatnajökull' model is extrapolated from the ICEMELT seismic refraction profile (Darbyshire *et al.*, 1998, 2000), and assumes a constant V_P/V_S ratio of 1.78. Depth is defined as below the average surface elevation of the two receivers nearest to the events, or approximately 700 m in this case (K. Vogfjörd and R. Slunga, personal communications). *– Einvítt P-hraðalíkan, Vatnajökulslíkanið, sem notað er við staðsetningar. Líkanið byggir á niðurstöðum úr ICEMELT verkefninu (Darbyshire og fleiri 1998, 2000) og gerir ráð fyrir V_P/V_S hlutfallinu 1,78. Dýpi miðast við tvær næstu stöðvar, sem eru í um 700 metra hæð á þessu svæði samkvæmt munnl. upplýsingum frá Kristínu Vogfjörð og Ragnari Slunga.*

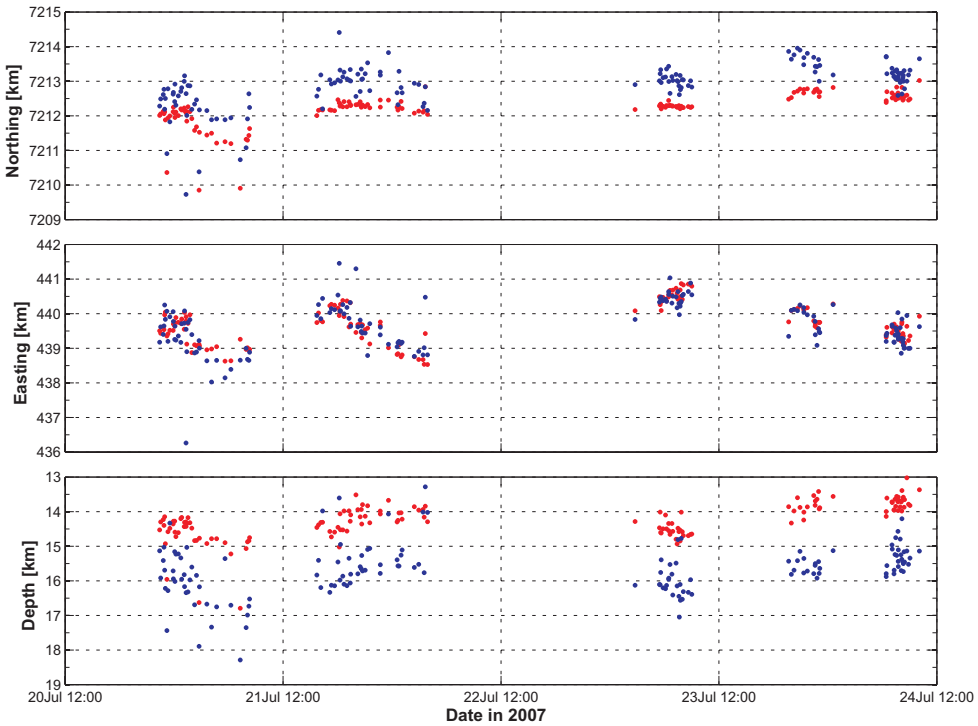

Figure 5. CMM automated locations (red) with respect to SIL-system catalogue locations (blue) in easting, northing, and depth. Hypocentre locations are plotted as reported directly from each system. For CMM, depths are reported below sea level; for the SIL-system on-line catalogue locations, depths are reported below the average elevation of the nearest one or two seismic stations to an event. Near Upptyppingar, the typical average offset for station elevation is 700 m. A correction in depth of this amount, however, does not account for all of the offset in depth (Table 1). SIL-system locations (derived using SIL data) appear deeper and northward of the CMM locations (derived using ASN data). – *CMM sjálfvirkar staðsetningar (rauðir punktar) í samanburði við yfirfarna SIL-skjálftalistann (bláir punktar). Gröfin sýna færslur til norðurs og austurs miðað við strikstefnu besta flatar í gegnum skjálftaþyrpinguna, ásamt dýpi sem fall af tíma. CMM staðsetningar eru miðaðar við sjávarmál, en SIL staðsetningar við meðalhæð næstu tveggja stöðva, eða um 700 m.y.s. Mismunandi hæðarviðmið skýrir ekki að fullu muninn á dýpinu (sjá töflu 1). SIL staðsetningar lenda dýpra og norðar en CMM staðsetningar með ASN netinu.*

II. Single-event locations

Secondly, we invert both SIL and ASN time-pick data using HypoInverse-2000 for a direct comparison of single-event locations. The SIL time-pick data is provided by the IMO in HypoInverse format, including both P- and S-wave onset times as well as pick weights for up to 18 SIL stations per event. Phase onset times and pick weights for the ASN data are selected in PPICK for up to 27 ASN stations (i.e., 21 Cambridge University and 6 SIL) per event. The results are presented in Figure 6, with each dataset plotted as depth below sea level. An offset between the SIL locations and the ASN locations of hundreds of metres in both northing and depth is evident (Table 1, second column). The minor difference in SIL catalogue locations derived by the IMO (Figure 5) relative to the SIL locations derived in HypoInverse-2000 (Figure 6) is attributed to different inversion programs and weighting schemes.

In an effort to distinguish the effect of network configuration from picking precision on absolute lo-

Table 1. Offsets in easting, northing, and depth of ASN locations relative to SIL locations. Relative displacements are calculated by comparing equivalent events on an event-by-event basis. The catalogue locations represent a comparison of CMM locations using ASN data with on-line SIL catalogue locations (first column). The large offset in depth is due in part to different definitions of zero-depth. For CMM, depth is defined as below sea level. For the SIL catalogue locations, depth is defined as below the nearest one or two seismic stations to an event. The single-event locations are derived by inverting IMO time picks of SIL data and Cambridge University time picks of ASN data in HypoInverse-2000 (second column). Offsets are also presented for HypoInverse-2000 location results using Cambridge University and IMO time picks for six SIL stations common to each network (third column). Overall, the offsets for locations using common stations are smaller than the offsets produced by network disparities. The offsets are not precisely zero owing to greater location scatter resulting from the use of fewer stations and also to minor differences in time picking. Lastly, offsets for relative locations determined by Cambridge University using HypoDD and the IMO using the software developed by Slunga *et al.* (1995) are presented (fourth column). These offsets are greater than those obtained by comparing Cambridge University results to IMO single-event locations relocated in HypoDD. The latter (i.e., +34 m, -344 m, and +649 m in easting, northing, and depth, respectively) more closely resemble the single-event location offsets (second column). – *Mismunur í staðsetningum með ASN netinu og SIL-kerfinu. Hliðrunin er fundin með því að bera saman reiknaðar staðsetningar hvers skjálfta fyrir sig. Tölurnar í fyrsta dálknum (Catalogue) sýna muninn á CMM staðsetningum í ASN netinu og daglegum jarðskjálftastaðsetningum úr SIL-kerfinu. Munurinn á reiknuðu dýpi er að hluta til vegna mismunandi viðmiðunar. Dýpið sem fengið er með CMM aðferðinni miðar við sjávarmál, en í SIL-kerfinu er miðað við hæð næstu jarðskjálftastöðva (um 700 metrar). Í dálki tvö eru bornar saman niðurstöður HypoInverse-2000 staðsetningar, úr SIL-kerfinu og ASN netinu. Í þriðja dálki eru bornar saman niðurstöður úr HypoInverse-2000 þar sem aðeins eru notaðar 6 SIL stöðvar. Minni heildarmunur er á staðsetningunum þegar notaðar eru sömu stöðvar og sama staðsetningarforrit. Mismunurinn skýrist af því að munur er á aflestrunum í kerfunum tveimur og að staðsetningaróvissan er meiri þegar færri stöðvar eru notaðar. Að lokum eru bornar saman niðurstöður úr afstæðum staðsetningum úr báðum kerfum, þar sem HypoDD er notað á aflestra Cambridgeháskóla úr ASN netinu, en aðferð Slunga og fleiri (1995) er notuð á SIL gögnin. Meiri munur er á þessum staðsetningum en þeim sem fást þegar aflestrar úr SIL kerfinu eru notaðir til að endurreikna staðsetningar með HypoDD. Í því tilviki er mismunurinn +34 metrar, -344 metrar og +649 metrar til austurs, norðurs og í dýpi, sem svipar til samanburðarins í dálki tvö.*

	Catalogue	Single-Event	Single-Event (6 SIL)	Relative Relocation
Easting (m)	-63	+31	-107	-530
Northing (m)	-647	-396	+170	-479
Depth (m)	+1246	+567	-180	+86

cations, we isolate and invert time-pick data from six SIL stations (VSH, ADA, HVA, BRU, MKO and KRE) that are common to both the ASN as well as the SIL network. The difference here is that the phase onset times and pick weights (for identical data from the same six stations) are determined independently: one set of time picks is selected by the IMO and the other set is selected through PPICK at Cambridge University. Each set of picks is passed through HypoInverse-2000 using the linear-gradient Vatnajökull velocity model and the single-event location results are presented in Figure 7.

Albeit scattered, the locations align well in easting, northing, and depth (Table 1), suggesting that picking precision is not a dominant factor in determining scatter and offsets in the hypocentres. The spatial errors for each set of time picks, as estimated by HypoInverse-2000, are equivalent within 100 metres (i.e., $\pm$0.8 km in the horizontal and $\pm$1.0 km in the vertical at one standard deviation). The eastward and southward shifts of the hypocentres relative to locations derived using the full networks (Figure 6) are attributed to an asymmetric, one-sided distribution of the six SIL stations about the earthquakes.

III. Relative Relocations

Finally, we compare SIL relative relocations with ASN relative relocations in Figure 8. SIL locations are provided by the IMO using the double-difference algorithm of Slunga *et al.* (1995) and ASN locations are derived using the double-difference algorithm of

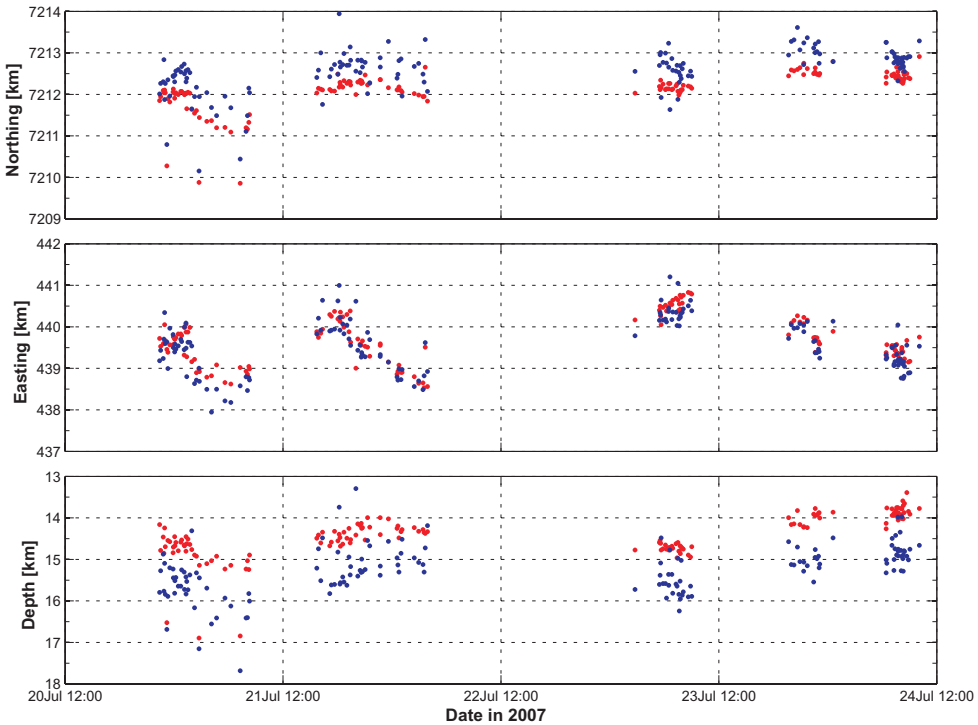

Figure 6. ASN single-event locations (red) with respect to SIL-system single-event locations (blue) in easting, northing, and depth. Here, travel times from each network are inverted using HypoInverse-2000 and the Vatnajökull velocity model (Figure 4). Furthermore, all locations have been re-datumed to depth below sea level. The time picks for the ASN are selected at Cambridge University using PPICK (Figure 3). The time picks for the SIL-system are selected at the IMO using similar manual refinement procedures. As with the catalogue locations (Figure 5), systematic offsets in northing and depth persist (Table 1). *– ASN staðsetningar á stökum skjálftum með komutímaaflestrum úr PPICK forritinu (mynd 3) (rauðir punktar), ásamt staðsetningum á stökum skjálftum með handvirkt leiðréttum komutímum úr SIL-kerfinu (bláir punktar). Í báðum tilfellum er notað staðsetningarforritið HypoInverse-2000 og Vatnajökuls-hraðalíkanið (4. mynd). Dýpið hefur verið leiðrétt, miðað er við sjávarmál. Eins og á 5. mynd má sjá kerfisbundna hliðrun til norðurs og í dýpi (tafla 1).*

Waldhauser and Ellsworth (2000) (i.e., HypoDD). All locations are redatumed to depth below sea level.

Each dataset exhibits well-defined, tightly clustered locations. It is interesting, however, that the offset in depth from the single-event locations (Figure 6) has all but disappeared (Table 1, second and fourth columns). Furthermore, the offset in easting has shifted by over 0.5 km with respect to the single-event locations. Here, the SIL relative locations have been provided directly by the IMO. When the SIL system time picks used to derive the single-event locations, however, are subsequently run through HypoDD, we do not find such a dramatic shift in the offsets. Indeed, we derive offsets that are very similar to those obtained when computing single-event locations.

IV. 3D Spatial Distributions

We now examine the distribution of hypocentres in three dimensions (3D) for SIL catalogue locations, SIL relative locations, and ASN relative locations by fitting the full dataset of 288 hypocentres to a plane using linear regression. Figures 9, 10 and 11 present the results looking along the strike direction of the

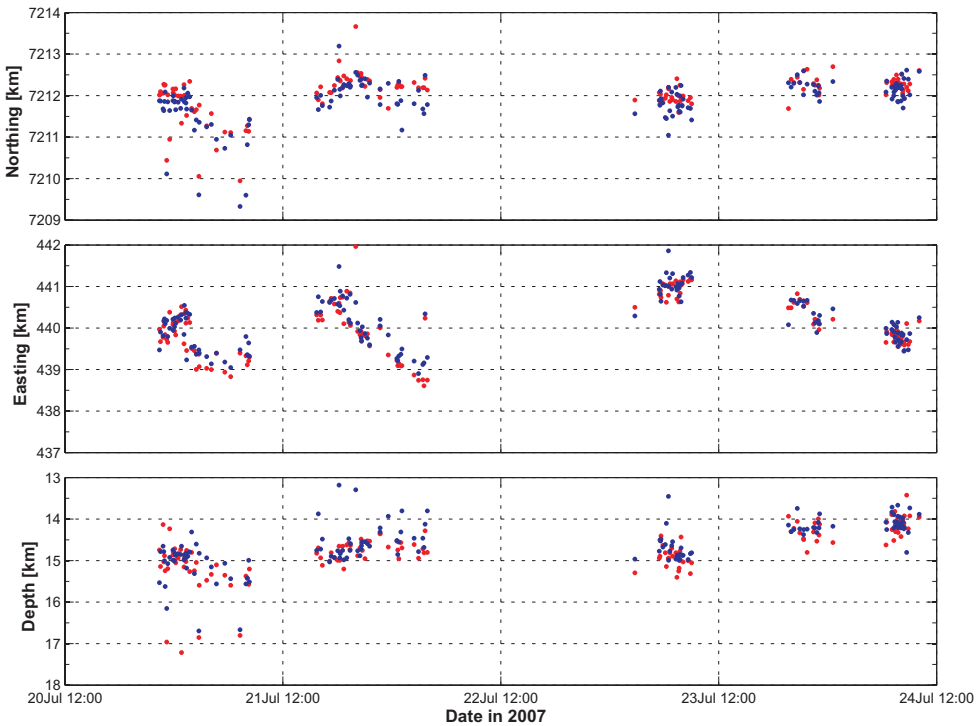

Figure 7. Single-event locations derived from the data of six SIL stations that are common to both the ASN and SIL-system. Locations are obtained from HypoInverse-2000 using time-pick information provided by Cambridge University from PPICK (red) and the IMO from similar manual refinement procedures (blue). All locations are re-datumed to depth below sea level. Due to the limited number of stations used here, the locations appear more scattered than in Figure 6; however, the offsets in northing and depth have effectively disappeared (Table 1). – *Staðsetningar stakra skjálfta með SIL-stöðvunum sex, sem notaðar eru í báðum netum. HypoInverse-2000 er notað í báðum tilfellum og komutímaaflestrar eru þeir sömu og á 6. mynd (PPICK og leiðréttir SIL-komutímar). Dýpið er miðað við sjávarmál í báðum tilfellum. Staðsetningarnar eru dreifðari en áður, vegna þess hve fáar stöðvar eru notaðar, en engin kerfisbundin hliðrun er sjáanleg.*

best-fit plane to each case, respectively. We have ignored events that locate below 17.5 km depth, as they do not seem to be associated with the dyke itself. These events are most apparent in Figure 11. The distribution of the hypocentres looking from the dip direction of the best-fit plane to the ASN relative locations is shown in Figure 12.

Two standard-deviation (2σ) relative location uncertainties for ASN are estimated as < 60 m, based on the output of HypoDD (Waldhauser, 2001), which computes errors using the method of singular value decomposition. Relative uncertainties for SIL are estimated as < 400 m by Jakobsdóttir *et al.* (2008); however, when SIL system time picks are applied through HypoDD for consistency with our own error estimates, we obtain relative location uncertainties of <120 m. Absolute horizontal and vertical uncertainties for the SIL catalogue locations are estimated as $\pm$0.7 km and $\pm$1.0 km (1σ), respectively (Slunga *et al.*, 1995).

The best-fit plane to the ASN data dips at 49.2°$\pm$0.2° (2σ) and strikes at N075°E$\pm$1°. For SIL, relative locations of identical events are best represented by a plane dipping at 45.6°$\pm$2.6° and striking

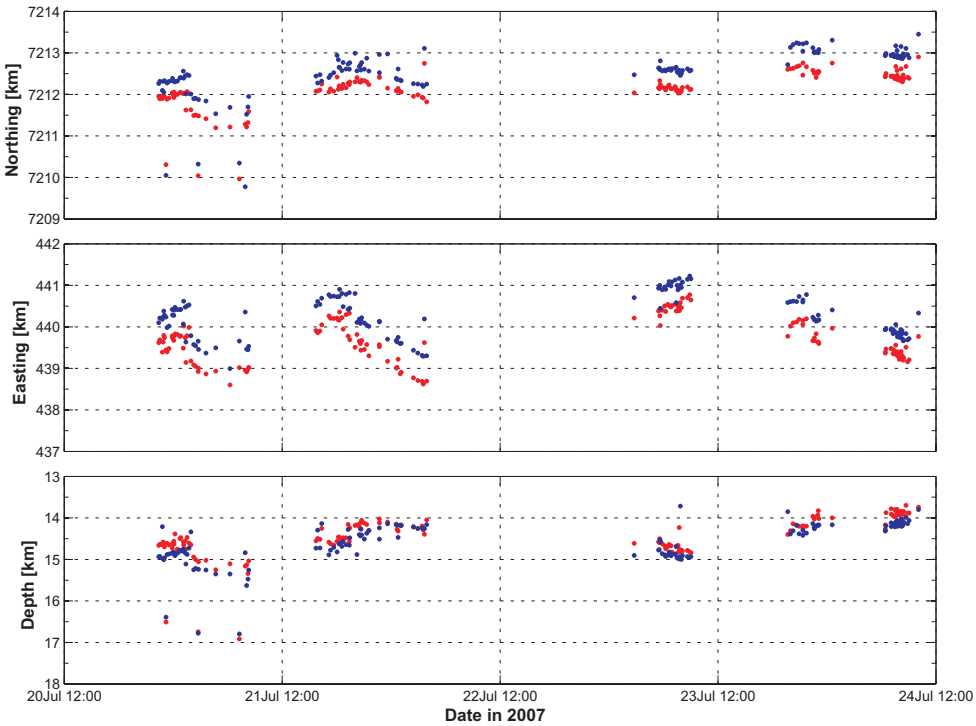

Figure 8. ASN double-difference relative locations (red) with respect to SIL-system double-difference relative locations (blue). The locations have been re-datumed to depth below sea level. Although the hypocentres are no longer as offset in depth relative to the single-event locations, an offset of ∼0.5 km in easting has appeared (Table 1). All hypocentres, however, are clustered considerably tighter than the single-event and catalogue locations. – *Samanburður á afstæðum staðsetningum (double-difference) úr ASN netinu (rauðir punktar) og SIL-kerfinu (bláir punktar). Dýpið er miðað við sjávarmál í báðum tilfellum. Munur á dýptarákvörðunum er minni en áður, en í staðin er um 0,5 km hliðrun til austurs, sem ekki sást áður (tafla 1). Upptök skjálftanna sýna nú mun minni dreifingu en þegar hver skjálfti er staðsettur fyrir sig.*

at N085°E±17°. Furthermore, for SIL catalogue locations that are routinely published on the IMO website, the hypocentres are fit by a plane dipping at 53.5°±21.8° and striking at N133E°±79°. The orientation of the best-fit plane to the catalogue locations is relatively unconstrained due to the considerable scatter in the hypocentres. Uncertainties are obtained through Monte Carlo simulations, in which each hypocentre is varied in a normal distribution about its initial location to the extent of the location errors. Standard deviations are then calculated from the distribution of best-fit planes. Since error estimates for individual events are not published with the on-line catalogue locations, we used error estimates provided directly by the IMO.

ASN double-difference relocations have a root-mean-square (RMS) misfit to the best-fit plane of only 135 m (114 m if the two off-axis points between 16.5 and 17.0 km depth are removed). This value is less than half of the SIL RMS misfit of 293 m and approximately twice the expected precision of relocations derived from ASN time picks at the 95% confidence level (i.e. 60 m). The RMS misfit for the on-line catalogue locations is 538 m. Characteristics of the best-fit planes are summarised in Table 2.

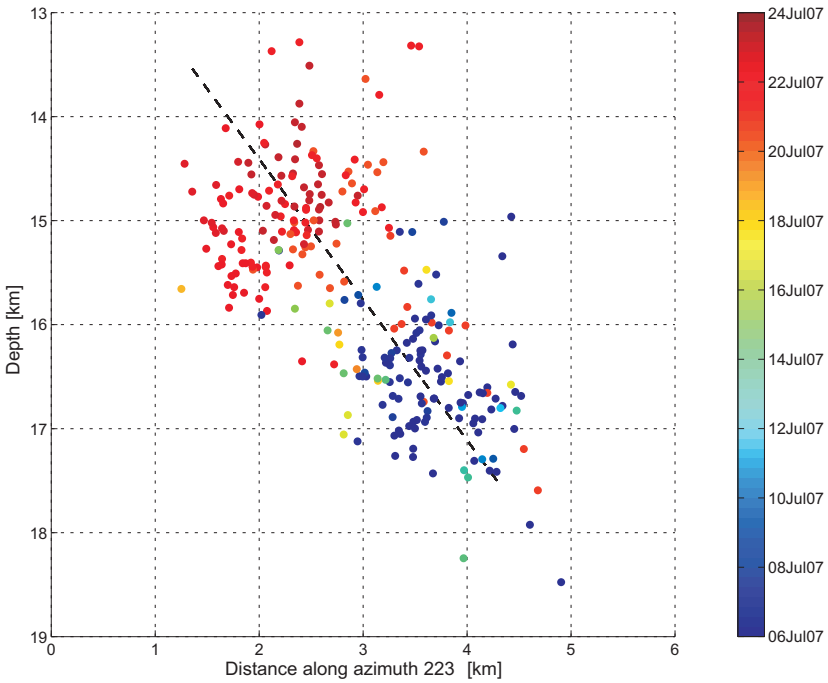

Figure 9. SIL-system catalogue locations fit to a plane using linear regression. The view is looking along the strike direction (azimuth 133°) of the best-fit plane to the catalogue hypocentres. Earthquakes are coloured by date and a dashed, black line depicts the plane. Due to the scatter in the locations (RMS misfit = 538 m), the orientation of the plane is not well defined (Table 2). – *Upptök jarðskjálfta samkvæmt yfirfarna SIL-skjálftalistanum og besta nálgun við tvívíðan flöt. Horft er eftir strikstefnu flatarins (133°). Litaskalinn sýnir upptakatímann og svarta strikalínan sýnir halla flatarins. Flöturinn er frekar illa skilgreindur vegna mikillar dreifingar á upptökum skjálftanna (RMS frávik = 538 m, tafla 2).*

Table 2. Plane parameters for the 6–24 July 2007 events derived from linear regression fits to SIL catalogue locations (SIL-Catal.), SIL relative relocations (SIL RR.), and ASN relative relocations (ASN RR.). – *Í fyrsta dálki er reiknuð stefna og halli flatar sem fellur best að staðsetningum í SIL-kerfinu á tímabilinu 6.–24. júlí 2007. Í öðrum dálki flötur sem passar við afstæðar staðsetningar í SIL-kerfinu og í þriðja dálki flötur sem passar við afstæðar staðsetningar í ASN netinu.*

	SIL Catal.	SIL RR.	ASN RR.
Strike (N°E)	133	085	075
Dip (°)	54	46	49
RMS Misfit (m)	538	293	114

As depicted by the colour bars in Figures 9–12, the overall seismic migration trend across the 288-event sequence is northward and to shallower depths. Individual clusters, however, exhibit significant lateral (E-W) movement as well (Figure 12). The 21–22 July cluster, for example, migrates nearly 2 km in ∼10 hours (Figure 8), corresponding to an average propagation rate of the hypocenters of up to 0.05 m s^{-1}.

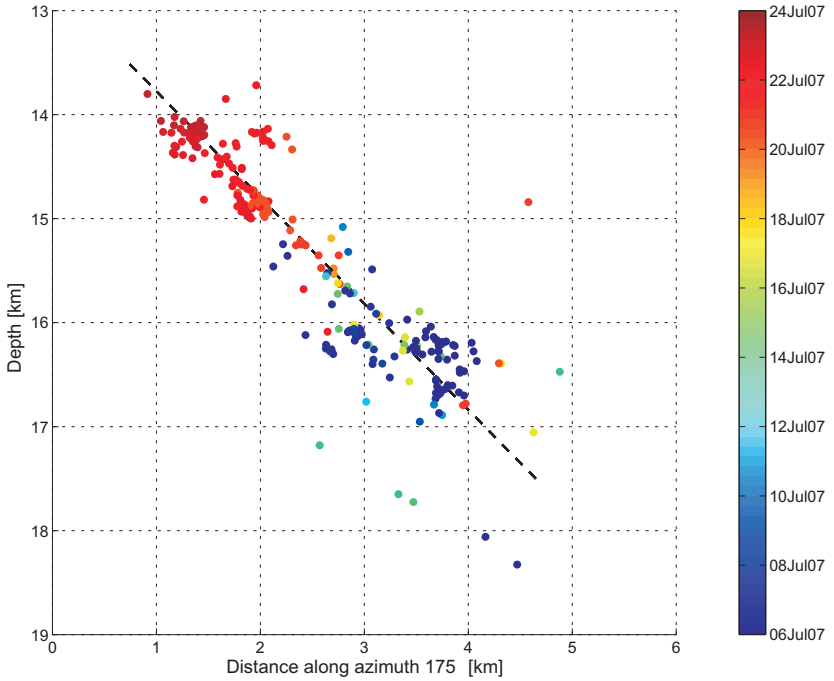

Figure 10. SIL-system double-difference relative locations fit to a plane using linear regression. A dashed, black line depicts the best-fit plane and the view is looking along the strike direction (Table 2). The RMS misfit to the plane is 293 m. – *Upptök jarðskjálfta samkvæmt afstæðum staðsetningum úr SIL-kerfinu og besta nálgun við tvívíðan flöt. Svarta strikalínan sýnir halla flatarins. Horft er eftir strikstefnunni (85°). Frávik skjálftanna frá fletinum (RMS) er nú 293 m (tafla 2).*

DISCUSSION

It is well known that factors such as network size and station distribution affect the accuracy of hypocentre locations (e.g., Bai *et al.*, 2006; Bondár *et al.*, 2004). Table 3 summarises the disparities between the ASN and SIL network sizes and geometrical configurations. The azimuthal gap provides a quantitative measurement of the extent to which events have occurred within the network. Smaller azimuthal gaps indicate denser networks with a preferable geometrical configuration.

Mean horizontal and vertical absolute location errors determined from all 288 single-event locations and as output by HypoInverse-2000 are included for comparison. Consistent with the double-difference relative location uncertainties, ASN single-event errors ($\pm$0.3 km and $\pm$0.5 km for horizontal and vertical errors, respectively) are improved by 40–50% over SIL single-event errors ($\pm$0.5 km and $\pm$1.0 km). Station distribution likely plays the main role as a comparison of locations based on IMO picks versus our picks for the same six stations yields similar results (i.e., $\pm$0.8 km and $\pm$1.0 km for the horizontal and vertical errors, respectively, for the same six stations but different time picks; see also Figure 7).

Particularly after relative relocation, SIL does a remarkable job considering the sparseness of the network. The orientation of the dyke plane is clear and migration patterns within swarms can be distinguished. One reason for the high quality performance of the SIL network relative to the denser, local ASN network is that the SIL system is not as sparse

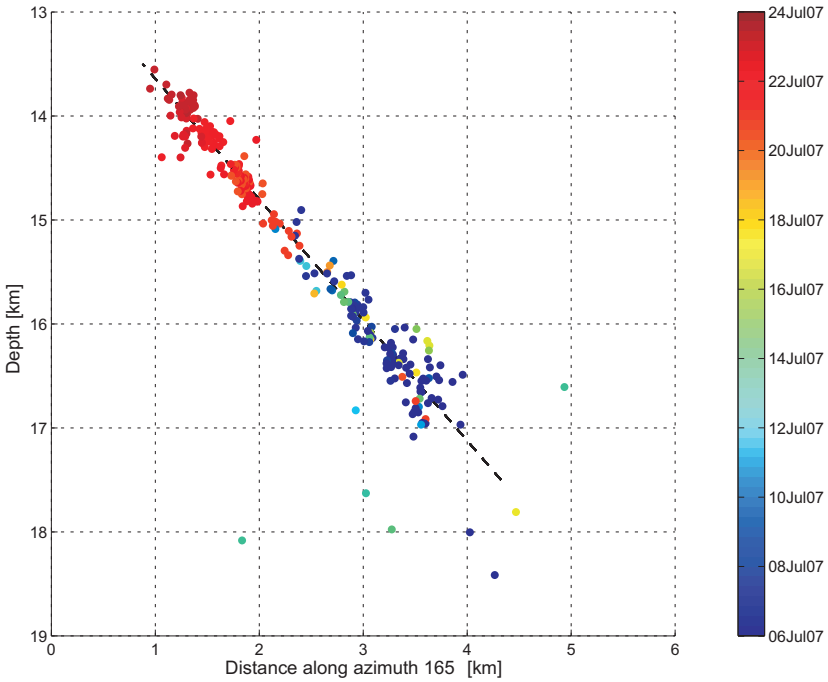

Figure 11. ASN double-difference relative locations fit to a plane using linear regression. A dashed, black line depicts the best-fit plane and the view is looking along the strike direction (Table 2). The RMS misfit to the plane is 135 m (or 114 m if the two off-axis points between 16.5 and 17.0 km are removed). Here the orientation of the plane (075/49) is well defined owing to the precise alignment of the hypocentres. – *Besta nálgun við tvívíðan flöt samkvæmt afstæðum staðsetningum úr ASN mælanetinu. Svört strikalína sýnir halla flatarins, horft er eftir strikstefnunni (tafla 2). Ferningsmeðaltal (RMS) fráviks við flötinn er 135 m (eða 114 m ef tveimur fjarlægum punktum á 16,5 og 17,0 km dýpi er sleppt). Flöturinn er vel skilgreindur með strikstefnu 75° og halla 49°.*

Table 3. Station coverage and absolute location uncertainties for the 6–24 July 2007 events derived from SIL and ASN single-event locations in HypoInverse-2000. – *Afstaða stöðva og óvissa í afstæðum staðsetningum jarðskjálfta á tímabilinu 6.–24. júlí samkvæmt SIL-kerfinu og ASN netinu.*

	SIL	ASN
Mean Azimuthal Gap (°)	135	82
Mean Distance to Nearest Station (km)	5.9	2.6
Mean Number of P/S Picks	16	42
Mean Absolute Horizontal Error (km)	0.5	0.3
Mean Absolute Vertical Error (km)	1.0	0.5

in the Upptyppingar area as in most regions of Iceland. This is due to the fortuitous installation of six nearby stations in 2004 to monitor the formation of the Hálslón water reservoir (Jakobsdóttir, 2008). All six SIL stations lie within 30 km of the Upptyppingar events. Moreover, SIL network stations are deployed in vaults whereas most of the Cambridge University instruments, intended for temporary deployment, were buried directly in sand, dirt and pumice. The SIL method of deployment reduces noise levels in the seismic signals, which allows for more precise time picking and locations.

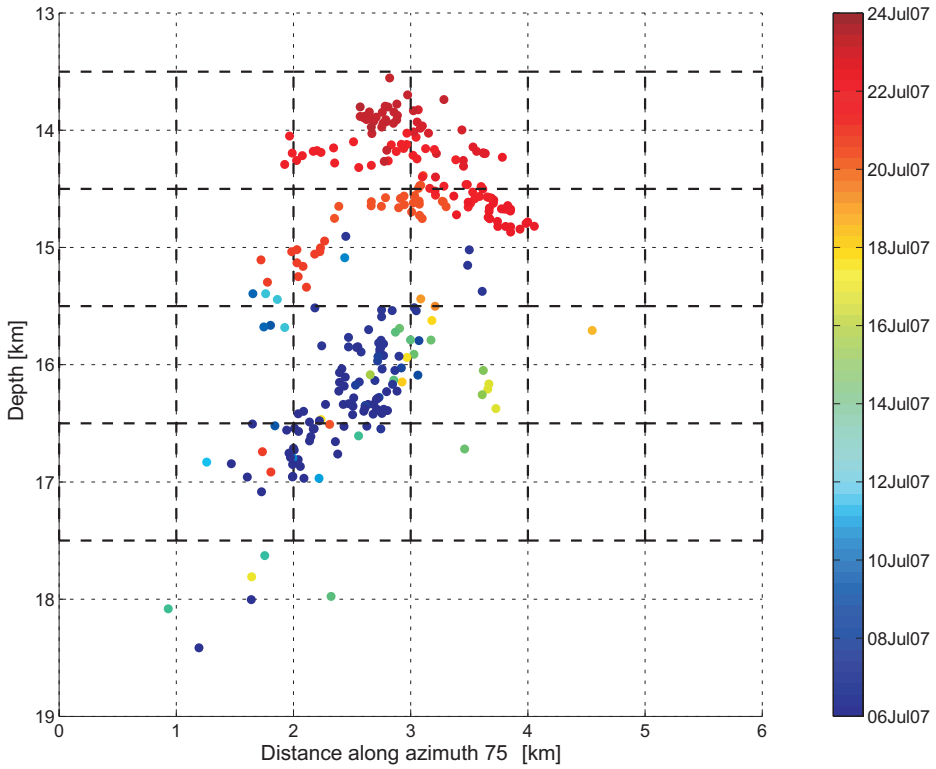

Figure 12. ASN double-difference relative locations looking from the dip direction of the best-fit plane to the hypocentres. Earthquakes are coloured by date allowing visualisation of the seismic progression along strike. – *Afstæðar ASN staðsetningar. Horft er þvert á strikstefnu besta flatar í gegnum þyrpinguna. Litaskalinn endurspeglar þróun virkninnar með tíma.*

Geophysical Interpretation

Melt injections at depth are not well documented observationally. As seismic swarms of the type observed near Upptyppingar are impossible to predict, observations and accurate locations of such events are dependent on serendipitous, a priori network placement. Although the SIL network captured the Upptyppingar events with an accuracy that allowed significant interpretation, details of the intrusion became lost in location ambiguities owing largely to a relatively sparse network. The dense seismic network deployed by Cambridge University around the nearby Askja volcano during summer 2007 supplied the additional spatial coverage needed to reveal fine morphological features of the intrusion, thereby permitting an improved investigation into its dynamics.

Brittle failure does not usually occur in the viscoelastic region of the crust, except where there are high strain rates (Rubin and Gillard, 1998). Hence, brittle failure in the middle to lower region of the crust is evidence for the presence of concentrated, high strain rates that might be melt-induced. Rubin and Gillard (1998) modelled the elastic stress field created by propagating fluid-filled cracks and concluded that most dyke-induced micro-earthquakes are likely to be the result of slip on existing fractures near the tip cavity of the dyke. Furthermore, they inferred the spatial distribution of the seismicity to represent stresses that are near to failure rather than delineating the extent of the dyke.

For micro-earthquakes of the magnitude observed at Upptyppingar, rupture diameters are on the order

of 100 m (Rubin and Gillard, 1998). Also, the two standard-deviation uncertainties in our relative relocations average to approximately 60 m. The RMS misfit to our best-fit plane (i.e., 114 m) is greater than the location uncertainty and earthquake rupture diameter; hence, the distribution of our hypocentral locations is amenable to some brittle fracture directly adjacent to the dyke, perhaps representing the ambient stress field that is near to failure. However, we do not observe widespread brittle deformation away from the dyke. Additional improvements to the analysis procedure and station configuration consistently reveal tighter clustering about the plane. We interpret this as evidence for minimal and localised brittle deformation surrounding the active dyke plane.

The tight spatial clustering revealed by the ASN locations also indicates that the seismicity progressed along the same dip throughout the study period. This is consistent with recent theoretical and experimental models of Maccaferri *et al.* (2010) that suggest it is energetically favourable for a dyke to continue to propagate along the same dip in a homogeneous, visco-elastic medium.

A detailed discussion of focal mechanisms is beyond the scope of this paper; however, we note that the 288 events consist of both reverse and normal faulting in an approximately 3:1 ratio. Moreover, an overwhelming majority of the events have inferred fault planes that are in alignment with the plane of the dyke (White *et al.*, 2011).

Although the Upptyppingar seismicity's tilted orientation, manifestation in the ductile zone of the crust, and concomitant dominance of high-frequency impulsive P-wave arrivals is unusual, the Lake Tahoe seismicity exhibited similar anomalous characteristics (Smith *et al.*, 2004). Linear regression models fit the seismicity beneath Lake Tahoe to a single planar structure dipping at 50° in visco-elastic crust.

Additional information regarding the presence of melt may also be obtained from the ratio of P-wave velocity to S-wave velocity (V_P/V_S), since the nature of the host material controls wave propagation rates. V_P/V_S ratios are derived independently for each of the 288 events using Wadati diagrams (Wadati, 1933) and PPICK-determined arrival times. Wadati diagrams display the time difference between the S-wave and P-wave arrivals against the arrival time of the P-wave for each station. For any given event, the slope of the best-fit line to the plotted station data represents the ratio of the P-wave to S-wave velocity minus one (i.e., V_P/V_S –1).

As depicted in Figure 13, two statistically significant populations emerge from the distribution of V_P/V_S ratios with hypocentral depth: one at <15.25 km depth with a mean V_P/V_S ratio of 1.78±0.02 (2σ) and another at 15.25–18.40 km depth with a mean V_P/V_S ratio of 1.80±0.03. Here, statistically significant refers to a rejection of the null hypothesis that the two populations are independent random samples from normal distributions with equal means but not necessarily equal variances at the 1% significance level, determined through a two-tailed t-test.

Waves produced by earthquakes at 15.25–18.40 km depth must pass through the overlying region of lower V_P/V_S; hence, it is possible to approximate the local V_P/V_S ratio of the deeper region. Assuming a two-layer model, with the average V_P/V_S ratio of the upper layer shallower than 15.25 km being 1.78 and a wave source at the centroid of the deeper cluster (∼16.3 km), we estimate the local V_P/V_S ratio of the deeper region to be ∼2.09. This is higher than that expected or measured for typical, solid high magnesian gabbroic rocks at mid-depth in the Icelandic crust (Christensen, 1996; Allen *et al.*, 2002; Bjarnason and Schmeling, 2009; Eccles *et al.*, 2009); hence, it is consistent with the presence of melt.

SUMMARY AND CONCLUSIONS

We have presented a test case that demonstrates the benefits of a dense, local seismic network for resolving fine morphological details within compact seismic swarms. However, we also show that high quality regional networks, such as the SIL system in Iceland, are more than sufficient for most interpretational requirements. Furthermore, we conclude that the network size and configuration dominate over the picking of phase arrivals in determining location accuracy and precision. This assumes, of course, that a reasonable effort has been made in picking phase arrivals. The IMO procedures as well as the techniques presented

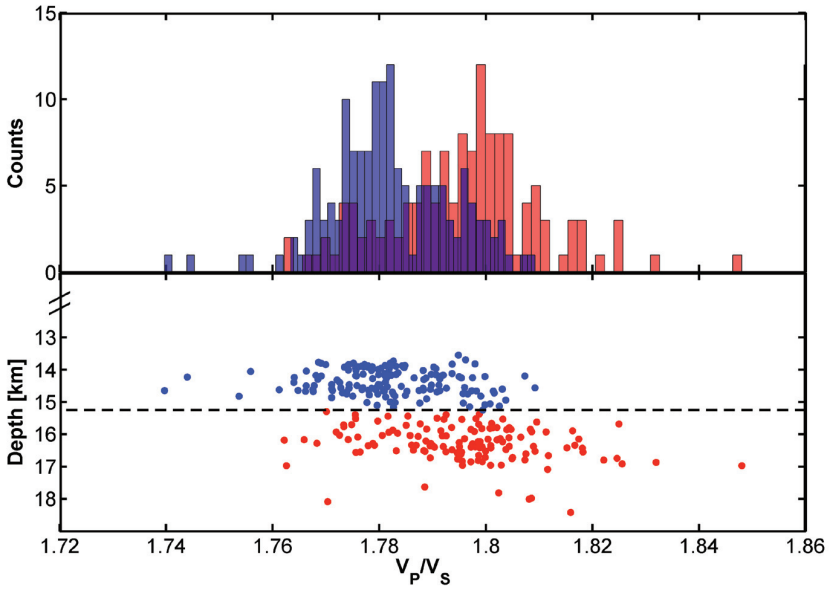

Figure 13. Seismic velocity V_P/V_S ratios as a function of depth. Blue colour represents the shallow population, which includes hypocentres that locate between 13.00 and 15.25 km below sea level. The deep population includes hypocentres that locate between 15.25 and 18.40 km below sea level and is shown in red colour. The histogram depicts a statistically significant bi-modal distribution of V_P/V_S ratios, representing the variation with depth.– *Hlutfall bylgjuhraða V_P/V_S sem fall af dýpi. Bláir punktar sýna grynnri þyrpingu með upptök á 13,00 til 15,25 km dýpi undir sjávarmáli. Upptakasvæði dýpri þyrpingarinnar er á 15,25 til 18,40 km dýpi og eru þeir skjálftar sýndir með rauðu. Súluritið sýnir marktækan mun á dreifingu V_P/V_S hlutfalls fyrir þessar tvær þyrpingar.*

in this manuscript include both automatic and manual quality checks that ensure precision phase-arrival selection. Relative relocation techniques also provide significant improvement in defining the spatial structure of the seismic swarms.

With respect to the Upptyppingar sequence, SIL locations define the general morphology of the dyke; however, high-precision locations reveal finer details of the kinematics of its propagation and evolution. The combination of a favourable network configuration and precision phase picking has revealed that any deformation off the plane of the dyke is not substantially greater than the uncertainty in the relative locations of the hypocentres. We interpret the incredible linear coherence of seismicity along the entire length of the dyke as evidence for minimal brittle deformation adjacent to the active dyke. This implies that melt-induced strain, at least for the 288 events examined here, is primarily compensated for viscoelastically, with only minor brittle fracturing occurring near the leading edge of the dyke or within the dyke itself.

We also note a relationship of V_P/V_S ratio with depth that is consistent with the presence of melt. This corroborates the interpretation that the spatially coherent Upptyppingar seismicity indeed delineates a melt intrusion at depth.

Acknowledgments

We thank G. B. Guðmundsson, B. S. Þorbjarnardóttir, and the Icelandic Meteorological Office (IMO) for providing data from six SIL stations, five of which are funded by Landsvirkjun-Power, for use in our analysis as well as the IMO-derived locations for all 2007 Upptyppingar events. We also appreciate the help of K. Vogfjörð and R. Slunga in clarifying the IMO single- and multi-event location techniques. Seismometers

for the ASN were borrowed from the Natural Environment Research Council SEIS-UK facility (loan 842). We thank M. Coffin, J. Eccles, D. Hawthorn, J.-C. Molina Santana, and A. Nowacki for their assistance with the fieldwork. We also acknowledge the helpful suggestions for improvement of the manuscript provided by I. Þ. Bjarnason and one anonymous reviewer. HRM gratefully acknowledges the financial support of the Marshall Aid Commemoration Commission. Dept. Earth Sciences Cambridge contribution number ESC1981.

ÁGRIP

Nákvæmni í staðsetningum á upptökum jarðskjálfta er meðal annars háð atriðum eins og fjölda og dreifingu mæla innan jarðskjálftamælanetsins og nákvæmni í aflestri bylgjufasa. Með þéttara neti fæst aukin staðsetningarnákvæmni sem gerir kleift að sjá fínni drætti í gerð jarðskorpunnar. Íslenska jarðskjálftamælanetið, SIL-kerfið, er hannað til að fylgjast í rauntíma með jarðskjálftavirkni undir landinu og notar til þess sjálfvirkan úrvinnsluhugbúnað. Í þessari grein eru niðurstöður úr SIL-kerfinu bornar saman við niðurstöður úr þéttara neti jarðskjálftamæla, sem rekið var tímabundið af vísindamönnum við Cambridge Háskóla, umhverfis Öskju og Herðubreið. Við vinnslu á gögnum úr þéttara netinu, sem kallast Askja Seismic Network (ASN), eru einnig notuð gögn frá 6 SIL-stöðvum. Í þessum samanburði eru notaðir 288 jarðskjálftar, sem áttu upptök sín við Upptyppinga á tímabilinu 6.–24. júlí 2007 og voru með skýr bylgjugögn. Skoðaðar eru niðurstöður sem fást með tveimur mismunandi aðferðum. Annars vegar eru skjálftarnir staðsettir einn og einn í einu og hins vegar er öll jarðskjálftaþyrpingin staðsett samtímis. Síðarnefnda aðferðin gefur mun nákvæmari innbyrðis afstöðu á milli skjálftanna (afstæðar staðsetningar).

Úr báðum netunum fæst mjög lík mynd. Hún sýnir að jarðskjálftaupptökin þyrpast um plan, sem samkvæmt þéttara netinu hallar u.þ.b. 49° til suðurs. Meðalfrávik skjálftaupptaka frá þessu plani er 114 m, sem er litlu meiri en staðsetningaróvissan (60 m). Reiknuð óvissa í ASN netinu er í bestu tilvikum aðeins um þriðjungur þeirrar óvissu sem reiknast með afstæðum staðsetningum í SIL-kerfinu. Þannig fæst nákvæmari mynd af planinu og því sem er að gerast í iðrum jarðar.

REFERENCES

Allen, R. M., G. Nolet, W. J. Morgan, K. Vogfjörd, M. Nettles, G. Ekström, B. H. Bergsson, P. Erlendsson, G. R. Foulger, S. Jakobsdóttir, B. R. Julian, M. Pritchard, S. Ragnarsson and R. Stefánsson 2002. Plume-driven plumbing and crustal formation in Iceland. *J. Geophys. Res.* 107, doi:10.1029/2001jb000584, 19 pp.

Bai, L., Z. Wu, T. Zhang and I. Kawasaki 2006. The effect of distribution of stations upon location error: Statistical tests based on the double-difference earthquake location algorithm and the bootstrap method. *Earth Planets Space* 58, e9–e12.

Bjarnason, I. Th. and H. Schmeling 2009. The lithosphere and asthenosphere of the Iceland hotspot from surface waves. *Geophys. J. Int.* 178, 394-418.

Böðvarsson, R., S. T. Rögnvaldsson, S. S. Jakobsdóttir, R. Slunga and R. Stefánsson 1996. The SIL data acquisition and monitoring system. *Seismol. Res. Lett.* 67, 35–46.

Böðvarsson, R., S. T. Rögnvaldsson, R. Slunga and E. Kjartansson 1999. The SIL data acquisition system – at present and beyond year 2000. *Phys. Earth Planet. Inter.* 113, 89–101.

Bondár, I., S. C. Myers, E. R. Engdahl and E. A. Bergman 2004. Epicentre accuracy based on seismic network criteria. *Geophys. J. Int.* 156, 483–496.

Brandsdóttir, B. and P. Einarsson 1979. Seismic activity associated with the September 1977 deflation of the Krafla central volcano in north-eastern Iceland. *J. Volcanol. Geotherm. Res.* 6, 197–212.

Christensen, N. 1996. Poisson's ratio and crustal seismology. *J. Geophys. Res.* 101, 3139–3156.

Darbyshire, F. A., I. Th. Bjarnason, R. S. White and Ó. G. Flóvenz 1998. Crustal structure above the Iceland mantle plume imaged by the ICEMELT refraction profile. *Geophys. J. Int.* 135, 1131–1149.

Darbyshire, F. A., K. F. Priestley, R. S. White, R. Stefánsson, G. B. Gudmundsson and S. S. Jakobsdóttir 2000. Crustal structure of central and northern Iceland from analysis of teleseismic receiver functions. *Geophys. J. Int.* 143, 163–184.

Drew, J., D. Leslie, P. Armstrong and G. Michaud 2005. Automated microseismic event detection and location by continuous spatial mapping. *SPE Annual Technical Conference and Exhibition*, Dallas, Texas, SPE 95513.

Drew, J. 2010. *Coalescence microseismic mapping: an imaging method for the detection and location of*

seismic events. PhD dissertation, University of Cambridge, 224 pp.

Eccles, J. D., R. S. White and P. A. F. Christie 2009. Identification and inversion of converted shear waves: case studies from the European North Atlantic continental margins. *Geophys. J. Int.* 179, 381–400.

Einarsson, P. and B. Brandsdóttir 1980. Seismological evidence for lateral magma intrusion during the July 1978 deflation of the Krafla volcano in NE-Iceland. *J. Geophys.* 47, 160–165.

Hasegawa, A., D. Zhao, S. Hori, A. Yamamoto and S. Horiuchi 1991. Deep structure of the northeastern Japan arc and its relationship to seismic and volcanic activity. *Nature* 352, 683–689.

Hjaltadóttir, S., K. Vogfjörð and R. Slunga 2009. Seismic signs of magma pathways through the crust in the Eyjafjallajökull volcano, South Iceland. *Icelandic Meteorological Office report* VÍ 2009–013, 33 pp.

Hooper, A., B. Ófeigsson, F. Sigmundsson, H. Geirsson, P. Einarsson and E. Sturkell 2009. Is magma generated due to retreating ice caps, likely to erupt? Constraints on lower-crustal stress in Iceland from InSAR. *Proceedings FRINGE Workshop*, Frascati.

Jakobsdóttir, S. S., M. J. Roberts, G. B. Guðmundsson, H. Geirsson and R. Slunga 2008. Earthquake swarms at Upptyppingar, north-east Iceland: a sign of magma intrusion? *Stud. Geophys. Geod.* 52, 513–528.

Jakobsdóttir, S. S. 2008. Seismicity in Iceland: 1994–2007. *Jökull* 58, 75–100.

Klein, F. W. 2002. User's guide to Hypoinverse-2000, a FORTRAN program to solve for earthquake locations and magnitudes. *U. S. Geol. Surv. Open File Rep.* 02-171, 1–123.

Maccaferri, F., M. Bonafede and E. Rivalta 2010. A numerical model of dyke propagation in layered elastic media. *Geophys. J. Int.* 180, 1107–1123.

Pedersen, R. and F. Sigmundsson 2004. InSAR based sill model links spatially offset areas of deformation and seismicity for the 1994 unrest episode at Eyjafjallajökull volcano, Iceland. *Geophys. Res. Lett.* 31, L14610.

Pedersen, R. and F. Sigmundsson 2006. Temporal development of the 1999 intrusive episode in the Eyjafjallajökull volcano, Iceland, derived from InSAR images. *Bull. Volc.* 68, 377–393.

Rubin, A. M. and D. Gillard 1998. Dike-induced earthquakes: Theoretical considerations. *J. Geophys. Res.* 103, 10,017–10,030.

Sigmundsson, F., S. Hreinsdóttir, A. Hooper, T. Árnadóttir, R. Pedersen, M. J. Roberts, N. Óskarsson, A. Auriac, J. Decriem, P. Einarsson, H. Geirsson, M. Hensch, B. G. Ófeigsson, E. Sturkell, H. Sveinbjörnsson and K. L. Feigl 2010. Intrusion triggering of the 2010 Eyjafjallajökull explosive eruption. *Nature* 468, 426-430.

Slunga, R., S. T. Rögnvaldsson and R. Böðvarsson 1995. Absolute and relative locations of similar events with application to microearthquakes in southern Iceland. *Geophys. J. Int.* 123, 409–419.

Smith, K. D., D. von Seggern, G. Blewitt, L. Preston, J. G. Anderson, B. P. Wernicke and J. L. Davis 2004. Evidence for deep magma injection beneath Lake Tahoe, Nevada-California. *Science* 305, 1277–1280.

Soosalu, H., J. Key, R. S. White, C. Knox, P. Einarsson and S. S. Jakobsdóttir 2010. Lower-crustal earthquakes caused by magma movement beneath Askja volcano on the north Iceland rift. *Bull. Volc.* 72, 55–62.

Stefánsson, R., R. Böðvarsson, R. Slunga, P. Einarsson, S. Jakobsdóttir, H. Bungum, S. Gregersen, J. Havskov, J. Hjelme and H. Korhonen 1993. Earthquake prediction research in the south Iceland seismic zone and the SIL project. *Bull. Seism. Soc. Am.* 83, 696–716.

Wadati, K. 1933. On the travel time of earthquake waves, II. *Geophys. Mag.* 7, 101–111.

Waldhauser, F. 2001. HypoDD: A computer program to compute double-difference hypocenter locations. *U. S. Geol. Surv. Open File Rep.* 01–113, 25 pp.

Waldhauser, F. and W. L. Ellsworth 2000. A double-difference earthquake location algorithm: Method and application to the Northern Hayward Fault, California. *Bull. Seism. Soc. Am.* 90, 1353–1368.

White, R. S., J. Drew, H. R. Martens, J. Key, H. Soosalu and S. S. Jakobsdóttir 2011. Dynamics of dyke intrusion in the mid-crust of Iceland. *Earth Planet. Sci. Lett.* in press.

Wright, T. J. and F. W. Klein 2006. Deep magma transport at Kilauea volcano, Hawaii. *Lithos* 87, 50–79.

Wright, T. J., C. Ebinger, J. Biggs, A. Ayele, G. Yirgu, D. Keir and A. Stork 2006. Magma-maintained rift segmentation at continental rupture in the 2005 Afar dyking episode. *Nature* 442, 291–294.